

Supplementary Information

Spatial Confinement of A Cationic MOF: SC-SC Approach for High Capacity of Cr(VI)-oxyanions in Aqueous Solution

Hong-Ru Fu^{ab}, Ning Wang^a, Jian-Hua Qin^a, Min-Le Han^{*a}, Lu-Fang Ma^{*a} and Fei Wang^{*b}

^a College of Chemistry and Chemical Engineering, Henan Province Function-oriented Porous Materials Key Laboratory, Luoyang Normal University, Luoyang 471934, P. R. China.

^b State Key Laboratory of Structural Chemistry, Fujian Institute of Research on the Structure of Matter, Chinese Academy of Sciences, Fuzhou, Fujian, 35002, China.

* Corresponding Author

Email:

minle_han@163.com.

mazhuxp@126.com

wangfei04@fjirsm.ac.cn

1. Materials and Instrumentation

All other chemicals were obtained from commercial sources and were used without further purification. Elemental analyses were carried out with a Vario EL III elemental analyzer. All powder X-ray diffraction (PXRD) analyses were recorded on a MiniFlex-II diffractometer with Cu-K α radiation ($\lambda = 1.54056 \text{ \AA}$) with a step size of 0.1° . Thermal stability studies were carried out on a NETSCHZ STA-449C thermoanalyzer with a heating rate of $5 \text{ }^\circ\text{C}/\text{min}$ under a air atmosphere. Inductively coupled plasma (ICP) measurement was performed on an Ultima-2 spectrometer. The Fourier transform infrared (FT-IR) spectra were performed on a Nicolet/Nexus-670 FT-IR spectrometer (KBr pellets, $4000\text{--}400 \text{ cm}^{-1}$).

2. X-ray diffraction analysis.

Suitable single crystals were carefully selected under an optical microscope and glued to thin glass fibers. Single-crystal X-ray structural analyses were performed on a XCalibur E CCD diffractometer with graphite monochromated Mo-K α radiation ($\lambda_{\text{mo-K}\alpha} = 0.71073 \text{ \AA}$) and Agilent Super Nova diffractometer ($\lambda_{\text{Cu-K}\alpha} = 1.54178 \text{ \AA}$) at 100 K. The structures were solved using the direct method and refined by full-matrix least-squares methods on F^2 by using the OLEX2.0 program package.¹ Non-hydrogen atoms were refined anisotropically. All the nonhydrogen atoms were refined with anisotropic parameters, while the H atoms were placed in calculated positions and refined using a riding model. Due to a bad disorder of the remaining anions and solvated water molecules in the crystal lattice, they were removed from the final refinement by SQUEEZE of the PLATON program.² CrO $_4^{2-}$ ions is disorder in the channels, the main interaction is static interaction, which was used to fix the free CrO $_4^{2-}$ ions. Totally, the thermal vibration factor of all O atoms is high. O9 and O10 come from the split atom, the occupancy is 0.5. O4 is located in the specific site of C2 axis, the occupancy is 0.5. CCDC:1479005 and 1854175 for **1** and **CrO $_4^{2-}$ @1**, respectively. Crystallographic data for four compounds were listed in Tables S1.

Crystal synthesis. Compound **1**. A mixture of TIPA (0.0225 g, 0.05 mmol), L-proline (0.0110 g, 0.11 mmol), $\text{Zn}(\text{NO}_3)_2 \cdot 6\text{H}_2\text{O}$ (0.0560 g, 0.2 mmol), MeOH (8 mL), and NaOH (2.1 mL, 0.1 M) was heated in a 20 mL scintillation vial at 100 °C for 72 h, followed by cooling to room temperature. Colorless rhombohedral crystals were picked and dried in air.

CrO₄²⁻@1. The crystals of as-synthesized compound **1** (20 mg) were immersed in a 20 mL 1×10^{-3} mol L⁻¹ solution of $\text{K}_2\text{Cr}_2\text{O}_7$ and kept for 6 days. After decanting the solution, the orange-yellow crystals were washed thoroughly with deionized water and dried in air.

The capture of in aqueous solution. All the tests were performed in aqueous solution. The UV-vis absorbance measurements were carried out periodically to monitor the adsorption process. The adsorption kinetics were tested by adding 50 mg compound **1** into 5 mL, 1.0×10^{-3} mol L⁻¹ $\text{K}_2\text{Cr}_2\text{O}_7$ aqueous solutions. The maximum capacity (saturation adsorption) of Cr(VI)-oxyanions was obtained through soaking 30 mg sample in 20 mL, 1.0×10^{-3} mol L⁻¹ $\text{K}_2\text{Cr}_2\text{O}_7$ aqueous solutions. Selective adsorption were checked in the presence of 1- and 10-fold molar of other anions (Cl^- , Br^- , SO_4^{2-} , ClO_4^- , BF_4^- , NO_3^-). The desorption experiments were carried out through adding the Cr(VI)-oxyanions-exchanged sample in the KNO_3 aqueous solution. The initial concentration of KNO_3 (100×10^{-3} mol L⁻¹) is 100-fold molar to that of $\text{K}_2\text{Cr}_2\text{O}_7$ (1.0×10^{-3} mol L⁻¹).

Table S1. The unit-cell parameters of sample 1 and CrO₄²⁻@1 .		
Framework	1	CrO ₄ ²⁻ @1
formula	C ₅₄ H ₅₃ N ₁₇ O ₁₆ Zn ₂	C ₁₀₈ N ₂₈ O ₁₄ Zn ₄ Cr ₃ H ₉₄
formula weight	1324.82	2489.51
crystal system	Monoclinic	Monoclinic
space group	C2/c	C2/c
<i>a</i> (Å)	30.9656(6)	30.349(12)
<i>b</i> (Å)	15.6428(3)	15.649(6)
<i>c</i> (Å)	29.8532(5)	30.830(13)
<i>α</i> (deg)	90.00	90.00
<i>β</i> (deg)	113.368(2)	113.410(18)
<i>γ</i> (deg)	90.00	90.00
<i>Z</i>	8	4
<i>V</i> (Å ³)	13274.5(5)	13437(9)
μ (Mo/Cu K α) (mm ⁻¹)	1.366	0.997
<i>F</i> (000)	4816	4928
temperature (K)	100	100
Theta min, max(deg)	5.1250, 74.4900	4.54, 54.84
<i>T</i> _{min} and <i>T</i> _{max}	0.782, 0.804	0.846, 0.896
<i>R</i> (int)	0.0245	0.0506
<i>N</i> _{ref} , <i>N</i> _{par}	13184, 725	14854, 725
^a <i>R</i> ₁ , ^b <i>wR</i> [<i>I</i> ≥ 2σ(<i>I</i>)]	0.0479, 0.1438	0.0965, 0.2572
<i>S</i>	1.071	1.062
<i>R</i> ₁ , <i>wR</i> ₂ (all data)	0.0583, 0.1531	0.1226, 0.2791
Reflns completeness	99.50	96.9
^a <i>R</i> ₁ = Σ <i>F</i> _o - <i>F</i> _c / Σ <i>F</i> _o . ^b <i>wR</i> ₂ = {Σ[<i>w</i> (<i>F</i> _o ² - <i>F</i> _c ²) ²] / Σ[<i>w</i> (<i>F</i> _o ²) ²]} ^{1/2} ; <i>w</i> = 1/[σ ² (<i>F</i> _o ²) + (<i>aP</i>) ² + <i>bP</i>] and <i>P</i> = (<i>F</i> _o ² + 2 <i>F</i> _c ²)/3.		

Notes: CrO₄²⁻ ions could be traced and confirmed via single-crystal to single-crystal (SC-SC) pattern. The number of chromates were defined completely in some structures, but not all chromates can be found in all exchanged crystals.

3. The experiment results and corresponding figures.

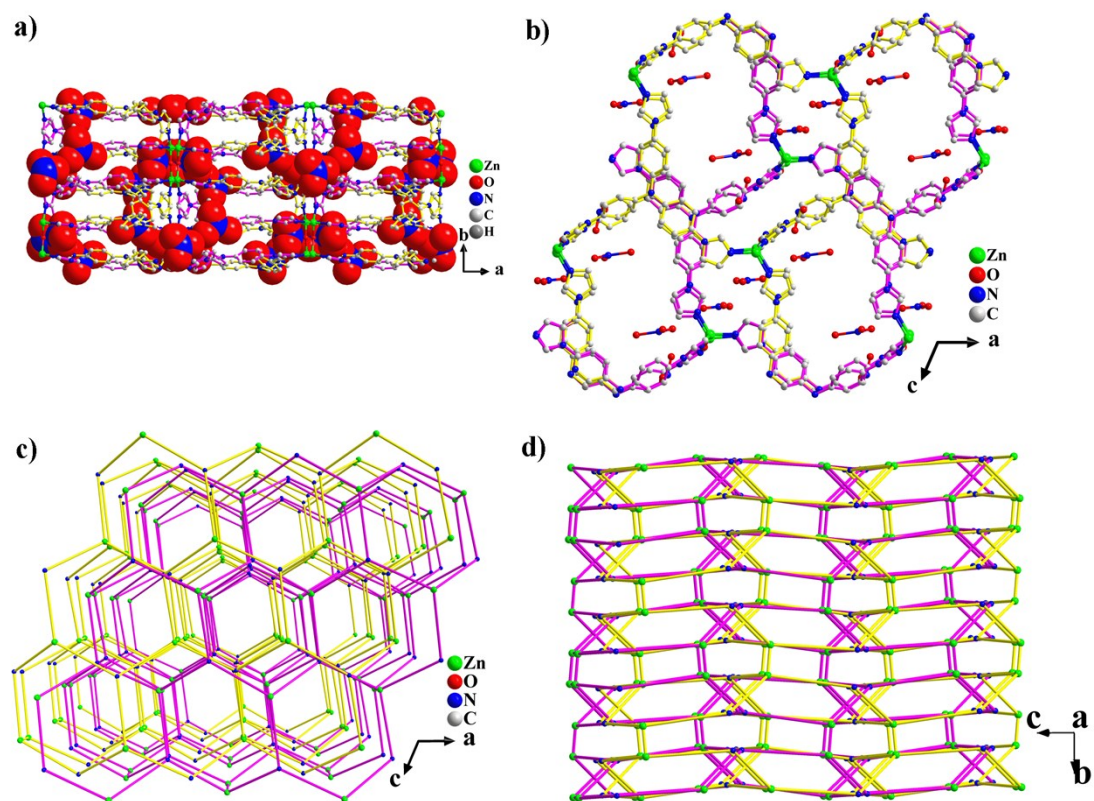


Fig. S1 (a) 3D structure of compound **1** along the c axis, NO_3^- ions as guests in the channels; (b) 3D structure of compound **1** along the b axis; (c) 3D topology of compound **1** along the b axis; (d) 3D topology of compound **1** along the a axis.



Fig. S2 The photograph of compound **1** before and after ion exchange in 15 ml, $1 \times 10^{-3} \text{ mol L}^{-1} \text{ K}_2\text{Cr}_2\text{O}_7$ solution. The adsorption process reached the dynamic balance state.

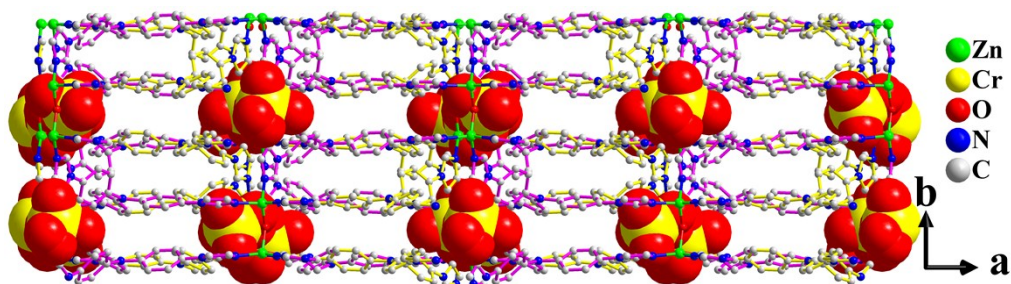


Fig. S3 (a) 3D structure of compound $\text{CrO}_4^{2-}@1$ along the c axis, CrO_4^{2-} ions as guests in the channels

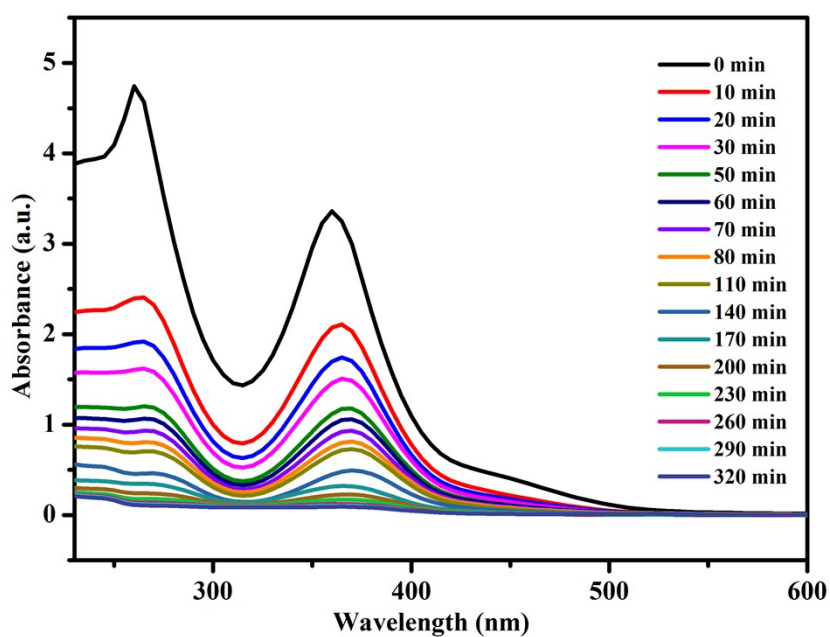


Fig. S4 UV-vis adsorption spectra of ion-exchange process for Cr(VI)-oxyanions capture, the initial concentration of $\text{K}_2\text{Cr}_2\text{O}_7$ solution is $1 \times 10^{-3} \text{ mol L}^{-1}$.

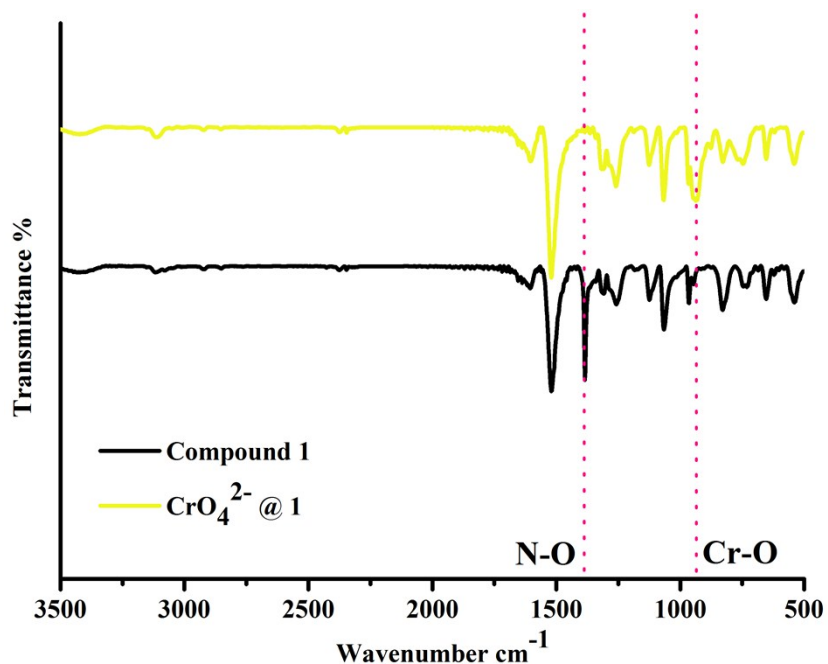


Fig. S5 IR spectra for: as-synthesized compound **1**. $\text{CrO}_4^{2-}@1$ was obtained in an aqueous solution of $\text{K}_2\text{Cr}_2\text{O}_7$ for 2 days. The peaks of NO_3^- significantly reduced, even disappeared, indicating that the NO_3^- ions were replaced by CrO_4^{2-} ions.

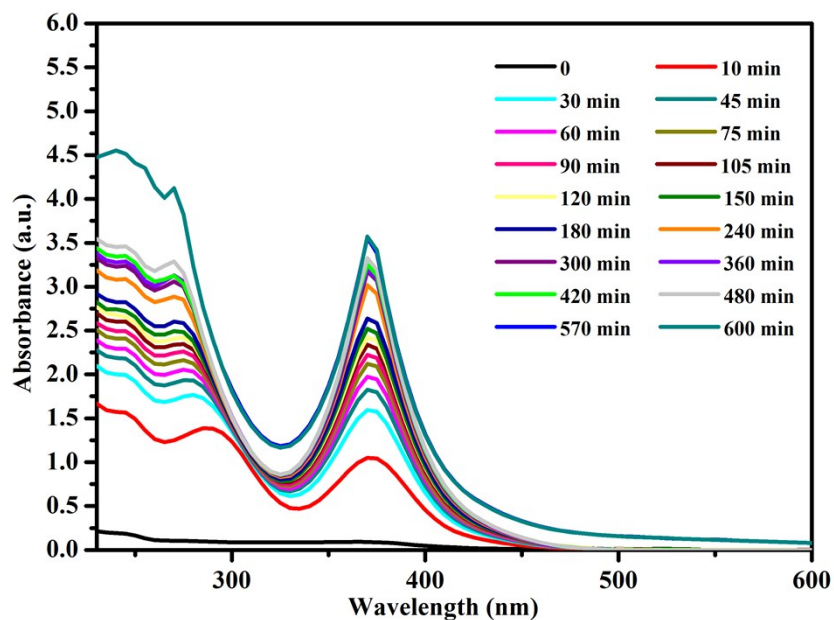


Fig. S6 UV-vis adsorption spectra of ion-exchange process for Cr(VI)-oxyanions releasing.

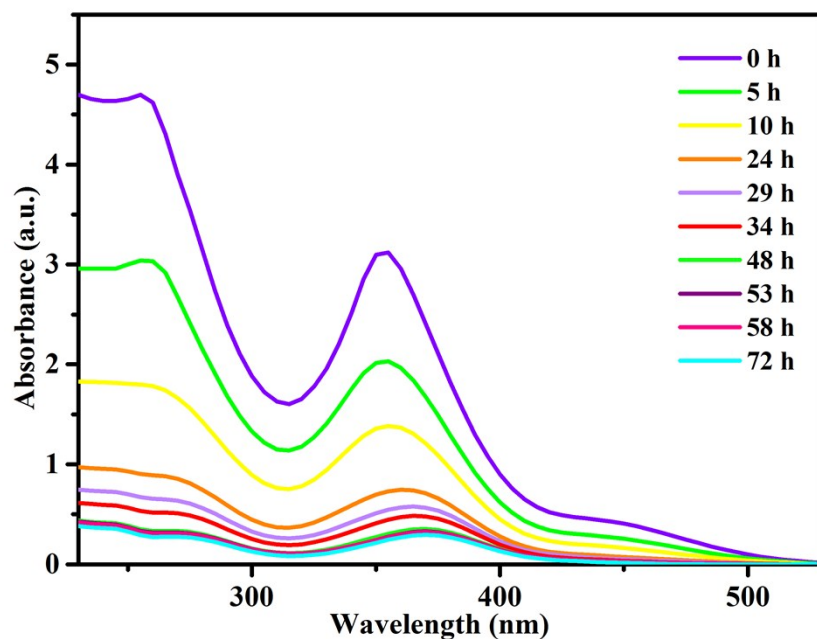


Fig. S7 UV-vis spectra of the adsorption process for Cr(VI)-oxyanions in 15 mL 1×10^{-3} mol L $^{-1}$. The adsorption process thoroughly completed after 72 hours. Based on Lambert-Beer law, the maximum capacity is 97.8 mg g $^{-1}$.

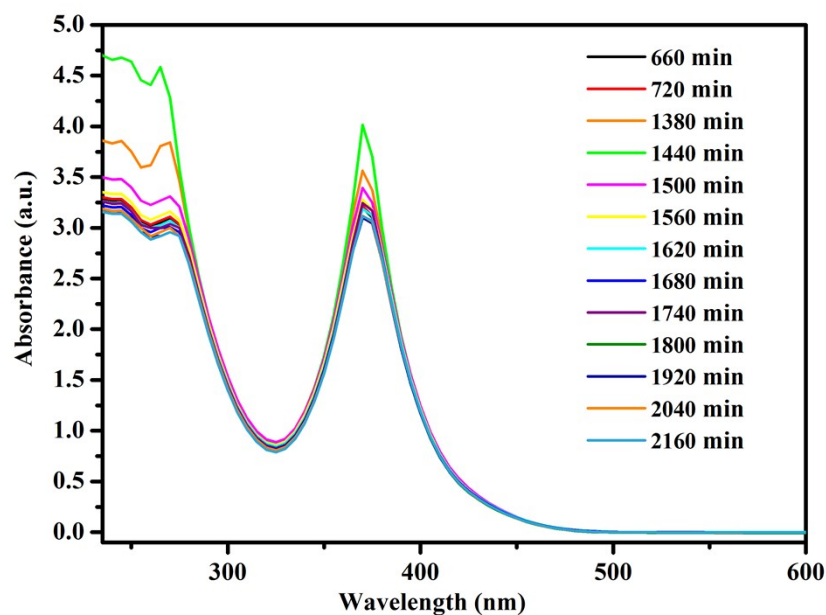


Fig. S8 Through the change of UV-vis adsorption spectra, it could be observed that with the continuing development of the ion-exchange process, CrO $_4^{2-}$ ions would replace NO $_3^-$ ions and return the framework. NO $_3^-$ ions replaced CrO $_4^{2-}$ ions from 660 to 1440 min, then CrO $_4^{2-}$ ions replaced NO $_3^-$ ions from 1500 to 1740 min, subsequently, NO $_3^-$ ions replaced CrO $_4^{2-}$ ions again from 1800 to 1920 min. Finally, the ion-exchange behaviors reach dynamic balance.

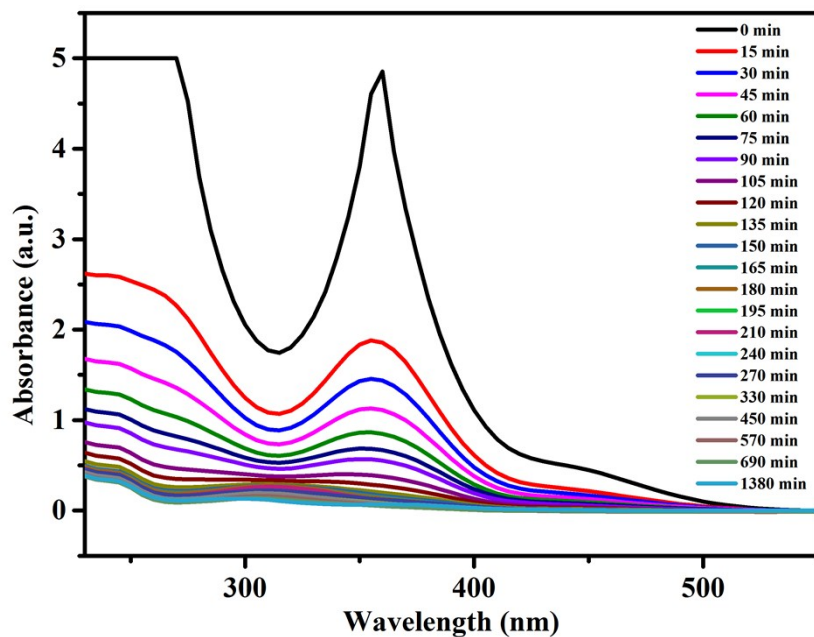


Fig. S9 The adsorption efficiency of **1** towards $\text{Cr}_2\text{O}_7^{2-}$ in the presence of interfering ions. The concentration of $\text{K}_2\text{Cr}_2\text{O}_7$ is $1 \times 10^{-3} \text{ mol L}^{-1}$. The concentration of the other ions (NO_3^- , ClO_4^- , Cl^- , Br^- , BF_4^- and SO_4^{2-}) is $1 \times 10^{-3} \text{ mol L}^{-1}$.

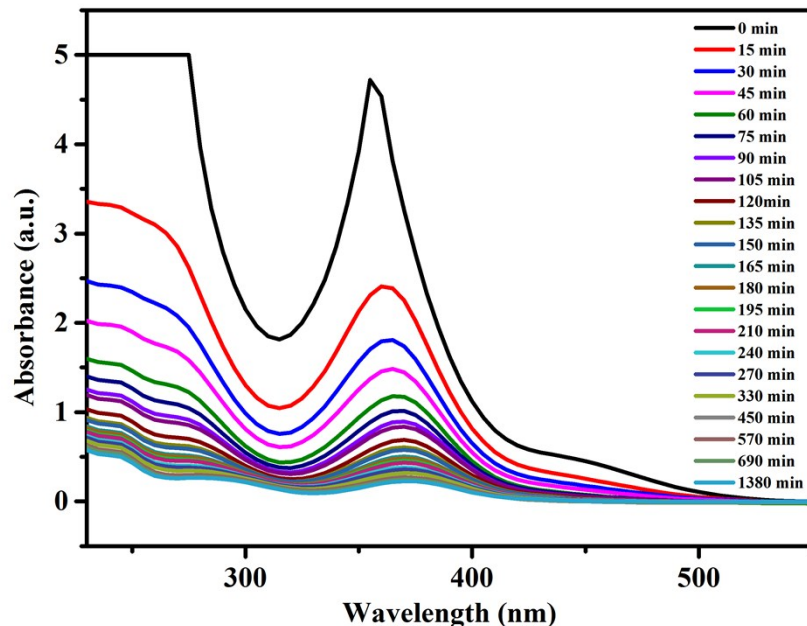


Fig. S10 The adsorption efficiency of **1** towards $\text{Cr}_2\text{O}_7^{2-}$ in the presence of interfering ions. The concentration of $\text{K}_2\text{Cr}_2\text{O}_7$ is $1 \times 10^{-3} \text{ mol L}^{-1}$. The concentration of the other ions (NO_3^- , ClO_4^- , Cl^- , Br^- , BF_4^- and SO_4^{2-}) is $10 \times 10^{-3} \text{ mol L}^{-1}$.

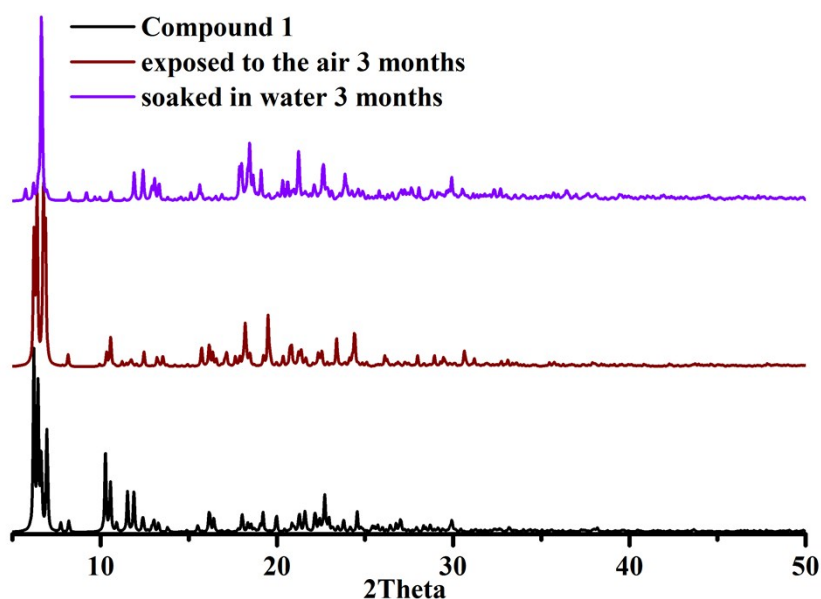


Fig. S11 Comparison of PXRD patterns of the series of compound **1** among as-synthesized one and compound **1** which was soaked in water or exposed to air.

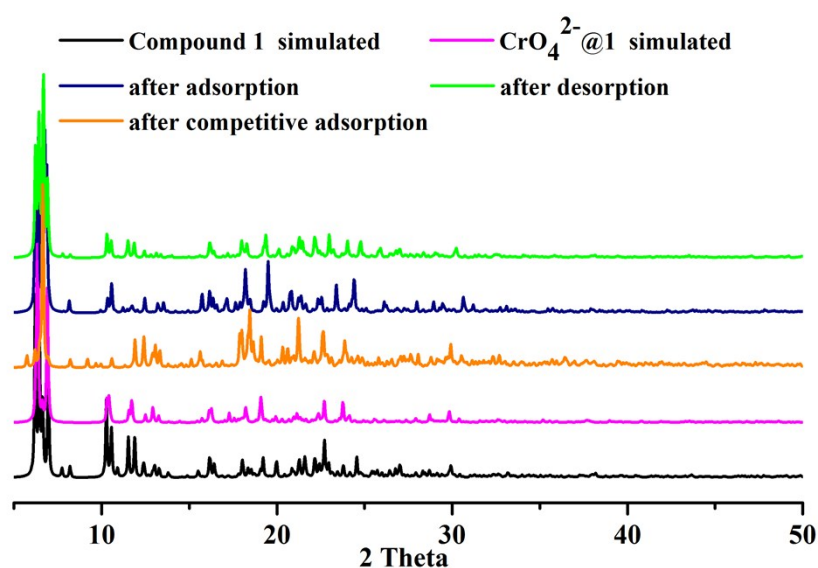


Fig. S12 Comparison of PXRD patterns of the series of compound **1** among as-synthesized one. The blue curve come from the sample which finished the adsorption process in the $1 \times 10^{-3} \text{ mol L}^{-1} \text{ K}_2\text{Cr}_2\text{O}_7$ solution. The green curve come from the sample which finished the desorption process in the $1 \times 10^{-3} \text{ mol L}^{-1} \text{ K}_2\text{Cr}_2\text{O}_7$ solution. The orange curve come from the sample which finished the adsorption process in the mixed solution. The concentration of anions is $1 \times 10^{-3} \text{ mol L}^{-1}$.

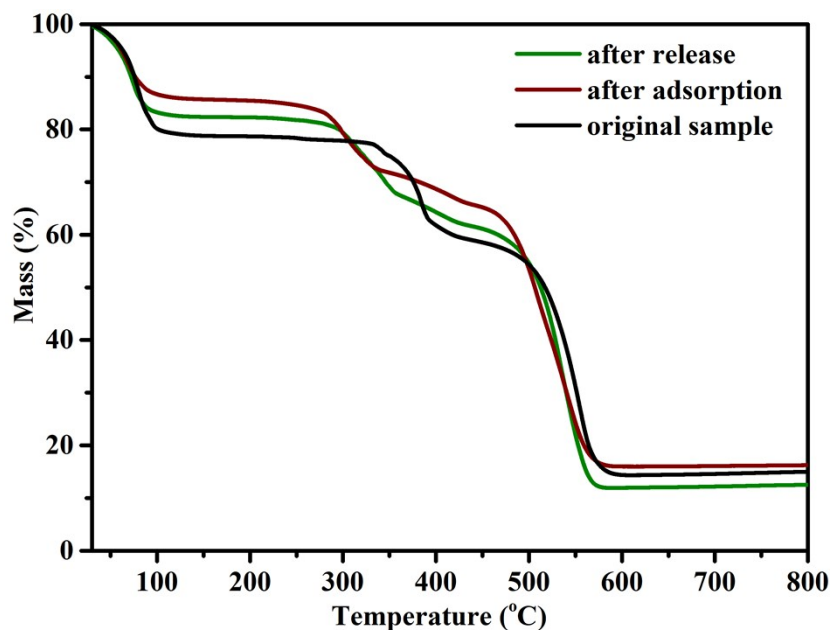


Fig. S13 TGA curves of the series of compound **1** under air atmosphere. The green curve come from the sample which finished the desorption process in the 5 mL, 1×10^{-3} mol L⁻¹ K₂Cr₂O₇ solution. The brown curve come from the sample which finished the adsorption process in the solution.

4. References

1. O. V. Dolomanov, L. J. Bourhis, R. J. Gildea, J. A. K. Howard, H. Puschmann, OLEX2: a complete structure solution, refinement and analysis program, *J. Appl. Crystallogr.*, 2009, **42**, 339–341.
2. A. L. Spek, PLATON SQUEEZE: a tool for the calculation of the disordered solvent contribution to the calculated structure factors. *Acta Crystallogr., Sect. C.*, 2015, **71**, 9–18.